Taylor & Francis
Taylor & Francis Group

Canadian Journal of Remote Sensing
Journal canadien de télédétection

ISSN: 0703-8992 (Print) 1712-7971 (Online) Journal homepage: https://www.tandfonline.com/loi/ujrs20

Large Area Mapping of Annual Land Cover Dynamics Using Multitemporal Change Detection and Classification of Landsat Time Series Data

Steven E. Franklin, Oumer S. Ahmed, Michael A. Wulder, Joanne C. White, Txomin Hermosilla & Nicholas C. Coops

To cite this article: Steven E. Franklin, Oumer S. Ahmed, Michael A. Wulder, Joanne C. White, Txomin Hermosilla & Nicholas C. Coops (2015) Large Area Mapping of Annual Land Cover Dynamics Using Multitemporal Change Detection and Classification of Landsat Time Series Data, Canadian Journal of Remote Sensing, 41:4, 293-314, DOI: 10.1080/07038992.2015.1089401

To link to this article: https://doi.org/10.1080/07038992.2015.1089401

Published online: 10 Oct 2015.

Canadian Journal of Remote Sensing, 41:293–314, 2015
ISSN: 0703-8992 print / 1712-7971 online
DOI: 10.1080/07038992.2015.1089401

Taylor & Francis
Taylor & Francis Group

Large Area Mapping of Annual Land Cover Dynamics Using Multitemporal Change Detection and Classification of Landsat Time Series Data

Steven E. Franklin[1], Oumer S. Ahmed[2*], Michael A. Wulder[3], Joanne C. White[3], Txomin Hermosilla[4], and Nicholas C. Coops[4]

[1]*Department of Environmental and Resource Studies/Science, Department of Geography, Trent University, Ontario, K9J 7B8, Canada*
[2]*Geomatics, Remote Sensing and Land Resources Laboratory, Department of Geography, Trent University, Ontario, K9J 7B8, Canada*
[3]*Canadian Forest Service (Pacific Forestry Centre), Natural Resources Canada, 506 West Burnside Road, Victoria, British Columbia, V8Z 1M5, Canada*
[4]*Integrated Remote Sensing Studio, Department of Forest Resources Management, University of British Columbia, 2424 Main Mall, Vancouver, BC V6T 1Z4, Canada*

Abstract. Land cover characteristics remain of particular interest to the monitoring and reporting communities, and approaches for generating annual maps of land cover informed by change information derived from long time series are critically needed. In this study, we demonstrate and verify the utility of disturbance and recovery metrics derived from annual Landsat time series to inform the classification of annual land cover over a > 1.2 million hectare forest management area in the Boreal Mixedwood Region of northern Ontario, Canada. Annual land cover maps were generated, producing temporally informed products and compared to the established approach of using single-date spectral variables and indices. The Random Forest (RF) classification algorithm was used to classify land cover annually between 1990 and 2010, followed by the application of an annual temporal filter to remove illogical land cover transitions. Change detection in the study area had an overall accuracy of 92.47%. The use of time series metrics in the classification of land cover improved overall accuracy by 6.38% compared to single-date results. Using a separate independent reference sample, the RF classification approach combined with postclassification transition filtering resulted in an overall classification accuracy of 87.98%. The use of annual change and trend information to guide land cover, which is further informed by logical land cover transition rules, points to the creation of efficient, robust, and reliable land cover products in a transparent and operational fashion.

Résumé. Les caractéristiques de la couverture terrestre sont intéressantes pour les communautés responsables de la surveillance. Le développement d'approches pour générer des cartes annuelles de la couverture terrestre qui sont informées par des informations de changements dérivées de longues séries temporelles est ainsi une nécessité cruciale. Dans cette étude, nous démontrons et nous vérifions l'utilité des mesures de la perturbation et de la récupération qui sont dérivées de la série temporelle Landsat annuelle afin d'informer la classification de la couverture terrestre annuelle pour une zone de gestion forestière supérieure à 1,2 million d'hectares dans la région de la forêt boréale mixte du nord de l'Ontario au Canada. Des cartes annuelles de la couverture terrestre qui fournissent des produits informés temporellement ont été générées et comparées à l'approche établie d'utiliser des variables et des indices spectraux à une date unique. L'algorithme de classification des Forêts Aléatoires «Random Forest» (RF) a été utilisé pour classer la couverture terrestre annuellement entre 1990 et 2010 et suivi par l'application d'un filtre temporel annuel pour enlever les transitions illogiques de la couverture terrestre. La détection de changements dans la zone d'étude avait une précision globale de 92,47%. L'utilisation de mesures de séries temporelles dans la classification de la couverture terrestre a amélioré la précision globale de 6,38% par rapport aux résultats à une date unique. En utilisant un échantillon de référence distinct et indépendant, l'approche de classification des RF combinée avec un filtrage de transition postclassification a abouti à une précision globale de classification de 87,98%. L'utilisation de l'information sur le changement et la tendance annuelle pour orienter la couverture terrestre, qui est en outre informée par des règles logiques de transition de la couverture terrestre, pointe vers la création de produits de couverture terrestre efficaces, robustes, fiables, de manière transparente et opérationnelle.

Received 20 Feburary 2015. Accepted 13 July 2015.
*Corresponding author e-mail: osahmed@trentu.ca

INTRODUCTION

The interpretation of annual land cover dynamics based on the analysis of remote sensing change detection and land cover

classification maps across large areas and long periods is an important natural resource management requirement (Lambin et al. 2003; Wulder and Franklin 2007; Roy et al. 2014). These activities are now feasible and facilitated by the free and open access to the entirety of the United States Geological Survey (USGS) Landsat archive (Woodcock et al. 2008) in a readily accessible form (Wulder et al. 2012). Access to this tremendously rich archive creates new opportunities for detecting vegetation changes at higher temporal frequency and at more detailed spatial scales than was previously possible in many areas (e.g., Huang et al. 2010; Kennedy et al. 2010; Zhu and Woodcock 2014), with Canada especially well represented by imagery (White and Wulder 2013). In actively managed forested areas, the annual assessment of Landsat time series data can be used to interpret detailed disturbance history and land cover changes (Sexton et al. 2013). Such an interpretation is also particularly useful in carbon modeling (e.g., Turner et al. 2004; Goward et al. 2008) and in characterizing forest change in a manner that is more consistent with detection of natural and human influences on ecological conditions and processes (e.g., Kennedy et al. 2014). Carbon balance, whether based on models or inventory, is highly dependent on the land cover because it affects several directly relevant characteristics such as albedo, emissivity, photosynthetic potential, and transpiration (Zhu and Woodcock 2014). Unique information produced from time series detection of change includes spectral clues on succession (Pflugmacher et al. 2012) and postdisturbance recovery (Hermosilla et al. 2015). Additionally, annual land cover information derived from Landsat can be used to produce a series of carbon model relevant variables such as predisturbance and postdisturbance land cover, which are also of general interest to monitoring, inventory, and reporting programs. This type of information is important in order to inform carbon models but conventionally difficult to derive when applying standard 2-date change detection and single-date land cover classification methods.

Annual land cover classification maps produced from dense Landsat time series data in specific areas enhance the interpretation of forest and land cover dynamics when used together with more spatially comprehensive, but often less frequently produced, Landsat-based single-image-date land cover products and compilations of multiple imagery (such as those used to create national or regional vegetation inventory data). For example, in Canada, among the most widely used national land cover maps is the Earth Observation for Sustainable Development of Forests product (typically referred to as EOSD LC 2000). This Landsat-based map provides a national land cover database of the forested area of Canada with 23 land cover classes for the year circa 2000. Annual land cover classification products are an ideal addition to the established EOSD LC 2000 maps, which have—in Canada and in similar large area coverages in other jurisdictions—been used to inform reporting programs (Wulder et al. 2004; Kangas and Maltamo 2006) and allow for the implementation of unique science activities (e.g., Wulder et al. 2011; Yemshanov et al. 2011).

Annual land cover classification using Landsat time series data has fostered the use of specific disturbance- or recovery-based metrics in the classification procedure (Hansen and Loveland 2012). Vegetation dynamics and forest cover changes identified using the "greatest change metric," or similar disturbance- or recovery-based metrics, attempt to identify vegetation dynamics that occur prior to the date of the image classification (e.g., Roy et al. 2014). The composition of land cover at any point in time is linked to its disturbance history. Therefore, inclusion of the disturbance-related variables is expected to increase the land cover classification accuracy over that which can be obtained using single-date spectral variables. In addition, by using the change metrics to inform the classification, it is possible to provide a single land cover class for a given pixel for the entire period when change is not specifically identified and there is no spectral evidence to indicate otherwise.

The use of these disturbance- or recovery-based metrics also implies an increment in the dimensionality of the datasets being used in image classification. This increase in dimensionality can compromise the capability of traditional multispectral classifiers but can be addressed by the selection of a robust classifier or an ensemble of machine-learning algorithms, such as the Random Forest (RF) package (Dietterich 2000). The RF approach, in particular, has received notable attention because it has flexibility with regards to the nature and distribution of input variables and has been found to be robust in situations problematic to traditional classifiers (Liaw and Wiener 2002). Recently, this has been buttressed in the use of disturbance- and recovery-based metrics extracted by time series trajectory-based methods to characterize forest change and estimate (via modeling) forest biophysical properties (Ahmed et al. 2015; Pflugmacher et al. 2012). The basic approach is based on detection of change in surface reflectance and classification of such changes in terms of land cover change or by characterizing trends (for more subtle discontinuous phenomena, such as partial land cover change or regrowth, see Meigs et al. 2011).

In this study, we present an approach for integrated change detection and land cover mapping with the aim of informing forest inventory and carbon accounting programs. Our method is novel in that it integrates: (*i*) annual large-area composites that contain no spatial or temporal data gaps; (*ii*) predictor variables that correspond with disturbance and recovery conditions; (*iii*) output as medium resolution annual land cover maps; and (*iv*) a Random Forest classifier that is robust in the case of heterogeneous classes and reference data error. Finally, we provide an indication of future improvements in the methods based on an analysis of both (*i*) land cover change over time, and (*ii*) other changes that are captured in the Landsat time series in related disturbance- or recovery-based metrics. This latter improvement will facilitate an interpretation of more subtle changes within a specific land cover, such as a pattern of smaller though still

significant changes, or through analysis of repeated land cover transitions (e.g., cyclical change).

DATA AND METHODS

In this study, we created and interpreted annual Landsat time series land cover classification and change detection maps that cover the period 1990–2010 in the Hearst Forest in northern Ontario, Canada. We incorporated various forest disturbance- and recovery-based metrics available from the image time series into the land cover classification process and created land cover change detection maps based on an analysis of the "greatest change" within the time series. We then developed a land cover transition matrix to relate the observed "greatest-change" locations to specific land cover changes, such as a change in conifer or mixedwood forest land cover subsequent to clearcut harvesting activities. To assess the accuracy of the change detection, we compared the results of these land cover change outcomes to an independent reference dataset created via visual interpretation of the Landsat time series imagery and aerial photography. The sampling design for selection of reference samples was a probability-based design such that the probability of selecting each land cover class is known and is sensitive to rare classes (Olofsson et al. 2014). The flowchart in Figure 1 summarizes the overall approach of this study described in the following subsections.

Study Area

The study area is the Hearst Forest Management Area located in northern Ontario (see Figure 2). This area is an actively managed, commercial forest that is found within the Boreal Mixedwood ecozone, and covers approximately 1.23 million ha (of which, approximately 1 million ha are productive forest; Hearst Forest Management Inc. 2011). The Hearst Forest is dominated by coniferous tree species, with black spruce *(Picea mariana* Mill. B.S.P.) representing 67% of gross volume in the area. Jack pine (*Pinus banksiana* Lamb.), white spruce (*Picea glauca* Moench Voss), balsam fir (*Abies balsamea* L. Mill.) and tamarack (*Larix laricina* Du Roi K. Koch) are also represented. Deciduous species in this region include white birch (*Betula papyrifera* Marsh.), trembling aspen (*Populus tremuloides* Michx.) and balsam poplar (*Populus balsamifera* L.). Approximately 60,000–70,000 ha of forest is harvested annually from this area using a variety of methods, including clearcutting (Hearst Forest Management Inc. 2007). With an active fire suppression program successfully controlling or limiting the effects of wildfire, timber harvesting is the most common form of disturbance in the Hearst Forest; however, large fires were recorded in 1995 and 1996. Insect outbreaks have also occurred in the area; for example, a spruce budworm outbreak occurred in 1999. Recent harvesting, fire history, and other disturbance events (e.g., insect outbreaks) in the area are described in the Hearst Forest Management Plan (2007–2017) published by Hearst Forest Management Inc. (2011).

Best-Available Pixel (BAP) Image Composites and Change Metrics

The Landsat imagery for the study area was obtained from the USGS Landsat archive. The study area intersects 6 Landsat WRS-2 path/rows. A total of 706 Landsat images, acquired between 1988–2012 and representing 1990–2010 conditions, were used to create multitemporal pixel-based image composites using a best-available-pixel (BAP) approach (implementing the methods described by White et al. 2014), and is briefly summarized here: First, atmospheric correction was applied to all images using the Landsat Ecosystem Disturbance Adaptive Processing System (LEDAPS) algorithm (Masek et al. 2006; Schmidt et al. 2013) transforming digital numbers into surface reflectance values. Second, clouds, cloud shadows, and water were detected and masked using the Function of mask (Fmask) algorithm (Zhu and Woodcock 2012). Once preprocessing was complete, candidate pixel observations were scored according to sensor, acquisition day of year (DOY), distance to clouds and cloud shadows, and atmospheric opacity. A target DOY of August 1 (Julian day 213) was selected within the growing season, and the date range for candidate images was restricted to $\pm$30 days. In the final step, the pixels with the highest score were used to populate the final image composite, and the surface reflectance values for these best observations were then written in the annual BAP composite. This method allows the production of spatially contiguous, cloud- and haze-free, spatially consistent temporal series of surface reflectance composites of Landsat data. Based on the rules applied, instances of no valid pixels for inclusion in the composite occurred. For example, pixel locations in the annual BAP composites with observations from images acquired outside $\pm$30 days of the target DOY were assigned a "no-data" value. Similarly, noisy or anomalous pixel values (spikes in the temporal pixel series) were also identified and assigned a no-data value as described in Hermosilla et al. (2015). In our study, infilling of data gaps (pixels with no-data values) was performed using the proxy value composite approach (Hermosilla et al. 2015). Briefly, this approach detects spectral change and derives a series of metrics characterizing these spectral changes and then uses these change metrics to aid in proxy value assignment. Here the greatest-change metric was used to flag disturbance events. Then, data gaps were filled by considering the full spectral information of the pixel time series; proxy values are informed by those from preceding and/or following dates, and these no-data pixels are replaced with values that are most spectrally similar in time and space. Replacement of these values is desired in order to enable production of gap-free, spatially exhaustive, annual proxy value composites that are spectrally consistent in order to support the production of annual land cover products. Our annual land cover classification was based on these proxy BAP composites and a series of disturbance- and recovery-based change metrics that were derived using a breakpoint detection process informed by the normalized burn ratio (NBR) on a temporal pixel series (as per Hermosilla et al. 2015). The breakpoint

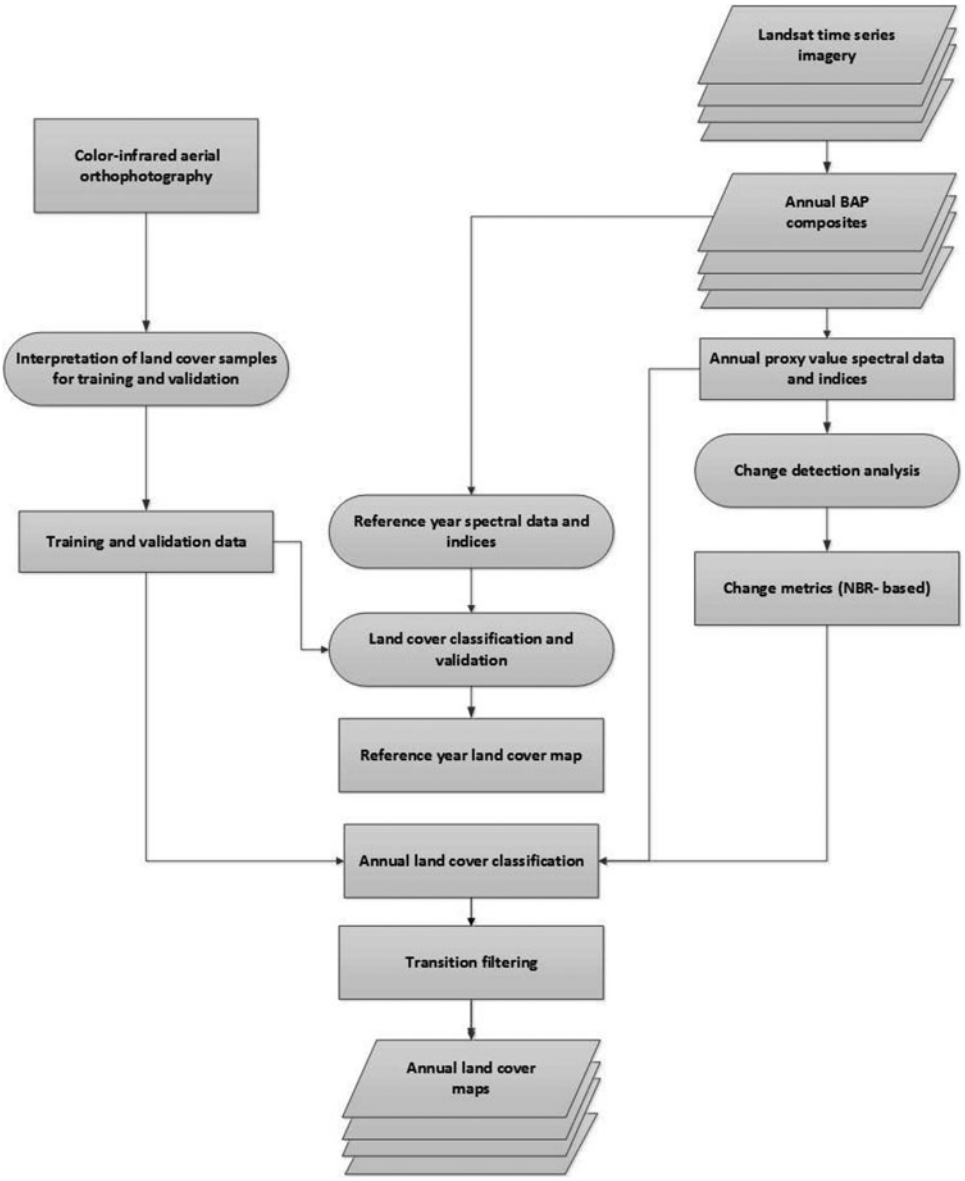

FIG. 1. A flowchart of the overall approach for the annual land cover classification.

detection process, in this study, is performed over the NBR pixel series, which has been demonstrated as sensitive and consistent for the retrieval of disturbance events over forest environments (Kennedy et al. 2010). The trends that can be computed after implementation of the breakpoint detection process are of distinct types. In this study, we used the "greatest negative change" in the time series to derive a set of descriptive change metrics. This greatest-change metric allowed us to characterize the change events as well as conditions pre- and postchange. The metrics relay information on change year, magnitude, and duration are grouped into prechange, at the time of change, and postchange categories. These change metrics characterize the negative breakpoint segments, using year, magnitude, and duration. Table 1 provides a complete listing, categorized by type, of all the spectral inputs derived from the BAP composites that were used as inputs for the land cover classification. Elevation information, derived from a digital elevation model (DEM), was the only noncomposite input data used for the classification.

Ancillary Data

There are several approaches for incorporating ancillary data in the image classification process based on earlier studies that incorporated DEM data into land cover classification (e.g., Janssen et al. 1990) to approximate differing ecosite conditions. In this study, several tiles of the Canadian Digital Elevation

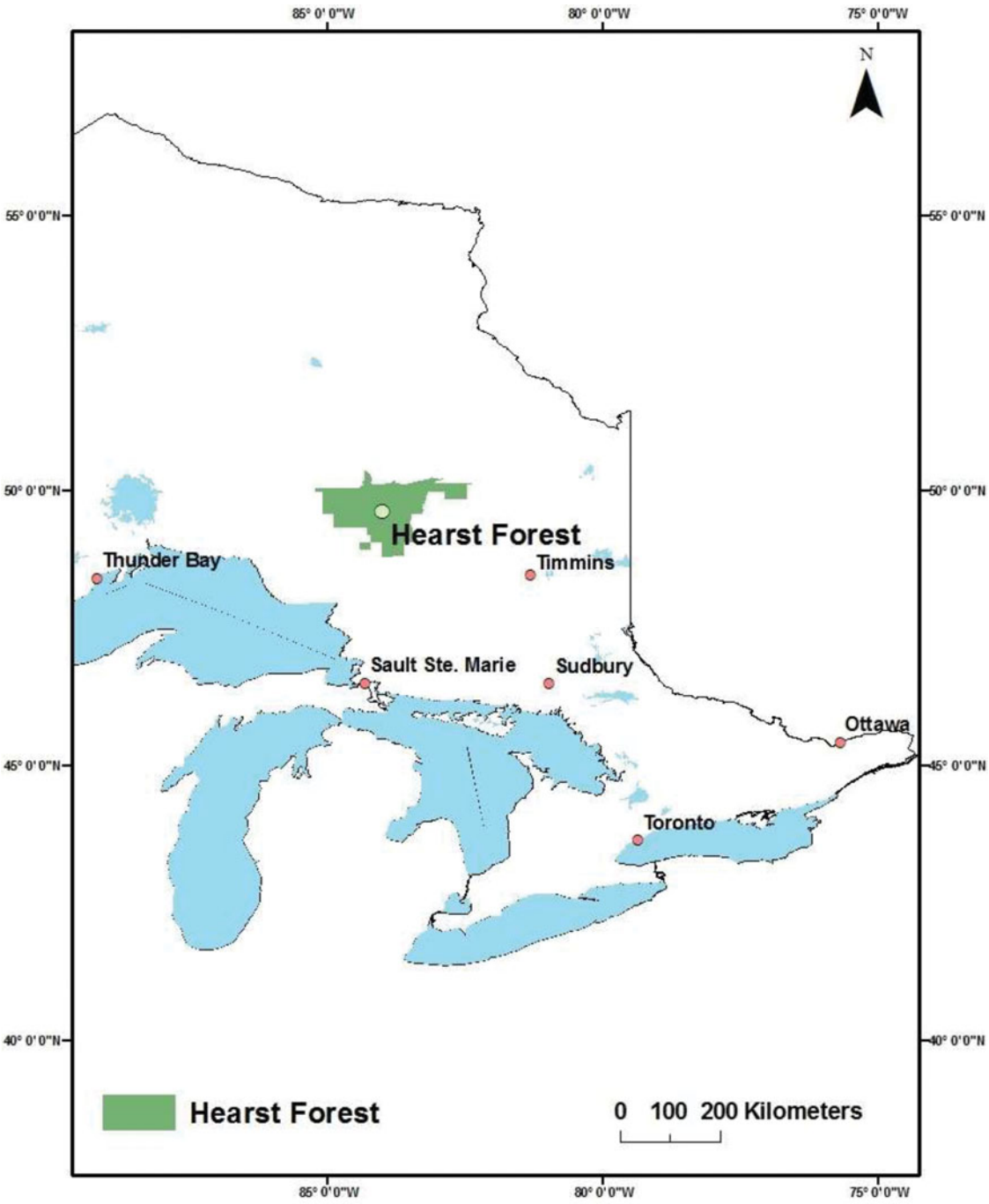

FIG. 2. The location of the study area within the Hearst Forest Management Area in northern Ontario.

Data (CDED) DEM were downloaded from the GeoBase online spatial data portal[1] to be used in the land cover classification.

High spatial resolution color-infrared leaf on aerial orthophotography was acquired in 2007 at approximately 1:20000 scale with 40 cm resolution covering most of the Hearst forest. This aerial orthophotography was used to collect calibration and reference data for each land cover class. An existing land cover product was used to provide strata for selection of calibration and reference samples. The EOSD LC 2000 is a land cover product representing the forested area of Canada circa 2000, with 23 land cover classes. Details on the land cover map can be found in

[1]www.geobase.ca

TABLE 1
Variables derived from the BAP composites that were used as inputs for the land cover classification; the first layer is elevation from the DEM, followed by 4 Landsat spectral bands, 2 proxy composite vegetation indices, and 14 NBR-based disturbance metrics derived from the Landsat time series

		Type	Variable	Description
Scenario 1: Single date inputs only	**Scenario 2: Single date inputs plus trajectory-based change metrics**	Topography	DEM	Digital Elevation Model
		Landsat spectral data	Red	Landsat Band 3
			NIR	Landsat Near Infrared (Band 4)
			SWIR	Landsat Shortwave Infrared (Band 5)
			SWIR	Landsat Shortwave Infrared (Band 7)
		Vegetation indices	NDVI	Normalized Difference Vegetation Index
			NBR	Normalized Burn Ratio
		Time series (NBR- based) disturbance metrics	Trend type	Characterize the type of trends according to: Monotonic trends (no change or breakpoint), single breakpoint or disturbed.
			NBR RSME	Root square mean error of fitting the trend to the observed pixel-series values
			Trend magnitude	Difference between the 1st and the last value of the fitted trends
			Greatest disturbance year	The year for the greatest disturbances
			Greatest disturbance magnitude	NBR variation during the disturbance segment
			Greatest disturbance duration	Persistence of the disturbance event
			Pre-disturbance magnitude	Variation of the NBR from the initial date to the disturbance
			Post-disturbance magnitude	Variation of the NBR from the disturbance to end date
			Pre-disturbance duration	Duration of the pre disturbance
			Post-disturbance duration	Duration of the post disturbance
			Pre-disturbance monotonic trend duration	Continual trends before the disturbance segment
			Post-disturbance monotonic trend duration	Continual trends after the disturbance segment
			Pre-disturbance monotonic trend magnitude	
			Post-disturbance monotonic trend magnitude	

Wulder et al. (2008). A stratified random sample was used with the EOSD LC 2000 map, providing an initial stratification to estimate the proportions of each land cover class over the entire area of the Hearst Forest in order to guide the proportion of training and reference samples (Wulder et al. 2006). Eight classes in the EOSD LC 2000 land cover map product were selected to characterize land cover in the Hearst Forest (mixedwood forest, coniferous forest, herb, wetland treed, broadleaf forest, wetland, water, and exposed land). These classes dominate the area per the EOSD land cover classification map product (note that these classes are derived from EOSD LC 2000 Level 4, which does not include forest density classes). Sampling strata were generated from the EOSD LC 2000 map, which enabled estimation of proportions of each land cover class over the entire area of the Hearst Forest to guide the sample composition and selection.

Change Detection Validation

The accuracy assessment of the change detection approach relied on independent reference data collected through visual interpretation of the Landsat time series imagery and the 2007 1:20000 scale color-infrared aerial photography. A stratified random sample design was used to select 100 samples (pixels) from the change and no-change strata, for a total of 200 reference pixels used to evaluate the accuracy of change detection. For each sample, the BAP composites were visually examined for the years immediately preceding and following the greatest-change year. In addition, the 2007 aerial photography was also examined, and the accuracy assessment results were recorded.

Land Cover Calibration and Validation

A stratified random sampling approach was used to acquire land cover classification calibration and reference data for each of the land cover stratum generated from the EOSD LC 2000 data. Sample size determination for reference purposes invariably involves trade-offs between the requirements of statistical rigor and logistical realities (Czaplewski and Patterson 2003; Wulder et al. 2007). The number of samples required for reference was determined using a 95% confidence interval for p with a margin of error of 5% and an assumption of 80% true accuracy (Cochran 1977; Wulder et al. 2007), resulting in a sample size of 174. Half of these samples were allocated proportional to the area of the classes (from EOSD LC 2000), whereas the other half were used to improve estimates for rare classes. For each sample, the land cover class in 2007 was interpreted from the aerial photography according to the same classification hierarchy as the EOSD product (Wulder et al. 2008). An additional 406 photo-interpreted samples were selected for model calibration and were allocated in the same manner (half proportional to the area of each EOSD class; half for rare classes; Table 2). All of the calibration and reference samples were selected in areas where land cover was unchanged throughout the period of the analysis (1990–2010).

TABLE 2
Number of calibration and reverence pixels for different land cover classes based on the EOSD LC 2000 land cover classification legend; samples were selected randomly and interpreted in the available color-infrared aerial orthophotography acquired in 2007

Class Name	Class Area (ha)	Calibration Sample Size	Reference Sample Size
Mixedwood	29919	138	59
Coniferous	21292	102	44
Herb	6424	40	17
Wetland treed	6220	39	17
Broadleaf	4778	33	14
Water	2671	24	10
Wetland	1008	17	7
Exposed land	296	14	6
Total		**406**	**174**

In this study, for accuracy assessment of change detection and land cover outputs, the approach that adjusts class area estimates for misclassification error was adopted as described by Card (1982) because it fits with recommended good practice for the accuracy assessment and use of land cover maps derived from remote sensing (Olofsson et al. 2013; Olofsson et al. 2014). In this approach, the misclassification-error-adjusted estimates of the area are derived from the confusion matrix, which forms the basis for the estimation of map accuracy.

Classification Algorithm

The Random Forest (RF) algorithm was selected because of its relatively high accuracy and computational efficiency (Brieman 2001). The dependent variable—one of the 8 classes—was predicted using the independent variables of Landsat spectral variables and indices, DEM and time-series metrics. The RF classifier consists of an ensemble of tree-based classifiers; it uses bootstrap samples with replacement to grow a large collection of classification trees, which assign each pixel to a class based on the maximum number of votes that a class receives from the collection of trees. Each tree is grown from a randomly and independently selected subspace (i.e., a certain proportion of pixels) of the measurement space (training pixels) that is used to train the RF classifier; the remaining samples (called out-of-bag cases) are used to assess the accuracy of the classification. Two parameters must be specified: (*i*) the number of trees to grow, and (*ii*) the number of randomly selected split variables at each node (mtry). The default number of trees (500) was used because values larger than the default are known to have little influence on the overall classification accuracy (Breiman and Cutler 2007). The other adjustable RF tuning parameter, the

TABLE 3
Accuracy assessment of change detection identified by the trajectory analysis for years between 1990 and 2010 based on 200 sample pixels examined in the image data and available color-infrared aerial orthophotography. Cell entries are expressed as the estimated area proportion of the cells of the error matrix

			REFERENCE			
		Change	No Change	Total	User's Accuracy	Commission Error
PREDICTED	Change	0.093	0.013	0.105	88.00%	12.00%
	No change	0.063	0.832	0.895	93.00%	7.00%
	Total	0.155	0.845	1		
	Producer's Accuracy	59.71%	98.50%	Overall Accuracy		92.47%
	Omission error	40.29%	1.50%	Margin of Error ±		3.66%

mtry parameter, controls the number of variables randomly considered at each split in the tree-building process, and is believed to have a "somewhat sensitive" influence on the performance of the RF algorithm (Breiman and Cutler 2007). For categorical classifications based on the RF algorithm, the default value for the mtry parameter is $\sqrt{p}$, where p equals the number of predictor variables within a dataset (Liaw and Wiener 2002). Model building and tuning were performed using version 3.0.3 of the 64-bit version of R (R Development Core Team 2014). Several add-on packages were used within R to create the final classification, which relied on the Random Forest package (Liaw and Wiener 2002; Breiman and Cutler 2007; Breiman 2001).

Reference Year Land Cover Classification

RF and the aforementioned calibration samples were used to produce a land cover classification for 2007. The 2007 reference date was selected based on the availability of near-coincident land cover validation data in the form of color-infrared aerial orthophotography at 1:20000 scale. Two different classification scenarios were explored (Table 1). In the first classification scenario, we used single-date spectral variables and derived spectral indices as inputs to RF. In the second classification scenario, we used the same set of single-date inputs as those used in Scenario 1, with the addition of change metrics derived from trajectory analysis of our stack of annual BAP proxy image composites (Tables 2 and 3).

Temporal Transition Filtering

The RF model with the greatest overall classification accuracy, as evaluated following the approach outlined previously, was applied to each year of the BAP proxy composite imagery. Postclassification, the annual land cover classifications were evaluated to identify and remediate illogical land cover transitions, using a temporal filter (e.g., Sexton et al. 2013). We defined illogical land cover transitions as those transitions that make no ecological sense in the context of the study area. An example of an illogical transition would be from coniferous land cover to exposed land cover to coniferous land cover in the span of only 3 years. The temporal filter was a 3-year moving window applied to each pixel through the time series, beginning in 1990 and proceeding annually to 2010. The filter was advanced year by year in the temporal sequence, and when an illogical transition was encountered, the land cover class from the previous year was automatically used to replace the current year's land cover. We then evaluated the impact that this postclassification temporal transition filtering had on the accuracy of the reference year land cover classification.

RESULTS AND DISCUSSION

Change Detection Validation

The accuracy of land cover change detection is reported in Table 3. Overall accuracy was 92.47% with a margin of error of ± 3.66%. Commission and omission errors for change events were 12.00% and 7.37%, respectively. Figure 3 shows all of the change events detected in the Hearst Forest for the period 1990–2010. Of the approximately 24 million pixels in the image of the Hearst Forest, approximately 2 million (or 10%) experienced a land cover change event during the 2 decades represented in the Landsat time series. The accuracy result indicates more omission errors than commission errors in detected changes. There is no noticeable trend in the spatial pattern of errors. The omission errors could result from partially changed pixels. Such pixels are usually difficult to detect, because the magnitude of change is mostly reliant on the proportion of change within that pixel.

Land Cover Validation

Two different land cover classification scenarios were explored for the 2007 reference year, using 2 different sets of input variables for modeling (Table 1). The 2007 classifications were validated using high-resolution color aerial photography

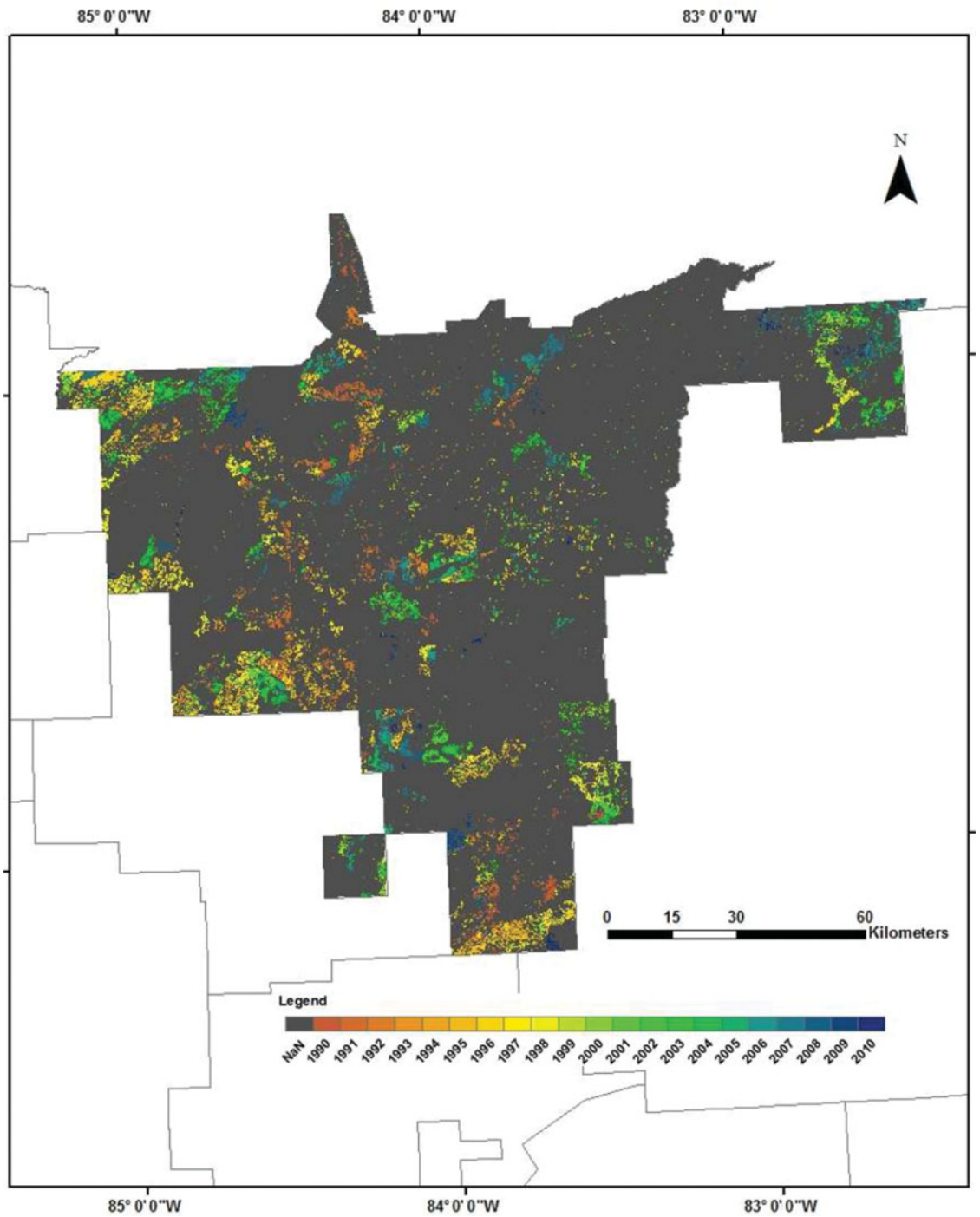

FIG. 3. Hearst Forest land cover change map showing land cover changes detected through greatest-change metric during 1990–2010.

acquired in 2007 and 174 reference samples. The accuracy assessment results for the first 2007 classification scenario, which used single-date inputs, are summarized in Table 4, and the results for the second scenario, which incorporated single-date inputs and time series change metrics are summarized in Table 5. Incorporation of the change metrics improved overall classification accuracy for 2007 from 79.38% to 85.77% and reduced the margin of error by 0.82%. Omission errors for Scenario 2 were lower for all classes except water and wetland, which were the same for both scenarios. The greatest decrease in omission error

in Scenario 2 relative to Scenario 1 were for the broadleaf and exposed land classes. Similarly, commission errors were lower for Scenario 2, particularly for the exposed land, wetland treed, and mixedwood classes. The mixedwood forest class, which represents approximately 41% of the Hearst Forest area, had an estimated user's accuracy of 84.75% for Scenario 2, compared to 71.88% for Scenario 1.

Based on these results, the Scenario 2 classification model was selected for application to all other years in the time series (1990–2010). Figure 4 shows the 2007 reference land cover classification map (Scenario 2) for the Hearst Forest with the 8 land cover classes. An estimate of variable importance (VI), as provided by the Random Forest algorithm, is shown in Figure 5. VI is estimated by randomly permuting the variable in the out-of-bag (OOB) samples; an increased OOB error is an indication of the importance of that variable to the model, providing indication of how influential an input variable is on the overall accuracy (Genuer et al. 2010). VI is measured with mean decrease in accuracy (MDA). To calculate the MDA of a variable, the values of the variable are randomly permuted for the OOB data, while keeping the values of the other variables constant. The importance of the variable is obtained by comparing the resulting misclassification rate with the rate achieved without randomly permuting the values of the variable. This procedure is repeated for each variable (Breiman 2001).

The top 5 most important variables were single-date Landsat spectral variables and spectral indices, with the next most important 3 variables selected from among the Landsat-based time-series change metrics (trend magnitude, greatest disturbance duration, and postdisturbance duration).

Final Classification and Land Cover Transitions

The annual land cover classifications were produced by applying the RF model developed in Scenario 2 for the reference year to all other years in the time series. Then, we examined all of the annual land cover classifications and assessed land cover transitions. Temporal transition filtering was performed to remove illogical class transitions, and the transitions that were considered illogical in the context of the study area are summarized in Table 6. The application of the filtering process allowed us to estimate the gain in classification accuracy from our post-classification transition-rule filtering. The accuracy assessment results for the 2007 filtered classification are summarized in Table 7. When compared to the results for the Scenario 2 reference classification for 2007 (Table 5), the overall accuracy was improved 2.2% as a result of the temporal transition filtering, whereas the margin of error was reduced by 0.36%. With the exception of the wetland treed and mixedwood classes, omission errors were the same or lower for the transition filtered classification, particularly for the wetland class. Commission errors were likewise reduced or remained the same for the filtered classification for most classes, but increased for wetland treed.

The time series of filtered annual land cover classifications were then used to characterize general land cover transformations in the Hearst Forest over the past 20 years. Figures 6, 7, and 8 illustrate examples of land cover transitions identified in the study; shown are the color-infrared aerial photography, NBR, land cover changes over the 1990–2010 time period, 8-class land cover classification for 2007, and a summary change transition map. Also shown in Figure 6 are 4 smaller sample sites (numbered 1–4), which are used in Figures 7 and 8 to illustrate different land cover change transitions in the study area.

Sites 2 and 4 were disturbed early in the time series 1991 and 1997, respectively; Sites 1 and 3 are more recent disturbances (2006 and 2005, respectively). These sites were selected to show typical land cover transition characteristics that are found in the study area. It can be seen from the summary land cover transition map (Figure 6) that many of the pixels that were disturbed early in the time series had recovered by the end of the time series. Of the approximately 10% of the study area that was identified as experiencing land cover change, more than 90% had recovered by 2010. The remaining areas show as herb or exposed land class in 2010 (See Figure 7). Examples of land cover transitions in areas shown in Figure 7a and 7b show Site 2 from Figure 6 in greater detail. Site 2 contains an area that was harvested at the beginning of the available time series; the dominant land cover class at the start of the time series was coniferous; as a result of harvesting, the majority of the area was converted to exposed land and then transitioned to herb, and eventually the site recovered to mixedwood. The graph in Figure 7b shows a pixel located near the edge of this harvest block (labeled as #1 in 7a) that transitioned from coniferous to exposed land then to herb and finally to mixedwood. Figure 8(a) and (b) show Site 3, which also displays a complex series of land cover transitions: the area was harvested in 2004 and 2005, and most of this area transitioned from exposed land (postharvest) to different land cover classes by the end of the time series in 2010. The graph (Figure 8b) shows an example of a pixel that was labeled as conifer at the beginning of the time series, was later classified as exposed land, and then experienced a transition over the next few years from herb to mixed wood.

Table 8 summarizes the land cover transitions in the Hearst forest, by 5-year epochs, from 1990 to 2010. These 5-year epochs were selected to illustrate broad land cover change patterns within the 20-year time interval examined for this study. Note that only pixels that changed land cover at some point–not necessarily from the beginning to the end of the time period, but at least once during the epoch–were tabulated in each epoch. Most land cover change pixels experienced only one land cover change in the 20-year time period. However, some pixels started a given epoch in 1 land cover class, changed to a different class, and then returned to the original class by the end of that 5-year epoch. The percentage of these pixels are counted in Table 8 as having changed from 1 class and returning to that class.

Approximately 10% of the study area (about 6000 hectare) are represented in these tables (i.e., areas that have experienced

TABLE 4

Error matrix of estimated area proportions for 8 EOSD LC 2000 land cover classes using single-date spectral variables and indices with 174 reference samples (interpreted in the available 1:20000 scale aerial orthophotographs). Cell entries are expressed as the estimated area proportion of the cells of the error matrix. Accuracy measures are presented with a 95% confidence interval

		REFERENCE										
	Class name	Mixedwood	Coniferous	Herb	Wetland Treed	Broadleaf	Water	Wetland	Exposed Land	Total	User's Accuracy (%)	Commission Error (%)
PREDICTED	Mixedwood	0.285	0.025	0.031	0.031	0.019	0	0	0.006	0.397	71.88%	28.13%
	Coniferous	0.042	0.278	0	0	0	0	0	0	0.320	86.96%	13.04%
	Herb	0.018	0	0.072	0	0	0	0	0	0.090	80.00%	20.00%
	Wetland Treed	0.018	0	0	0.050	0	0	0.005	0	0.073	68.75%	31.25%
	Broadleaf	0.005	0	0	0	0.050	0	0	0	0.055	90.91%	9.09%
	Water	0	0	0	0	0	0.039	0	0	0.039	100.00%	0.00%
	Wetland	0	0	0	0.002	0	0	0.014	0	0.016	85.71%	14.29%
	Exposed Land	0	0	0.004	0	0.001	0	0	0.005	0.009	50.00%	50.00%
	Total	0.368	0.303	0.107	0.083	0.070	0.039	0.018	0.011	1		
	Producer's accuracy (%)	77.43%	91.83%	67.55%	60.08%	71.97%	100.00%	75.05%	43.27%	Overall accuracy		79.38%
	Omission error (%)	22.57%	8.17%	32.45%	39.92%	28.03%	0.00%	24.95%	56.73%	Margin of Error ±		6.01%

TABLE 5
Error matrix of estimated area proportions for 8 EOSD LC 2000 land cover classes using combination of single-date spectral variables and time series disturbance metrics with 174 reference samples (interpreted in the available 1:20000 scale aerial orthophotographs). Cell entries are expressed as the estimated area proportion of the cells of the error matrix

		REFERENCE										
	Class name	Mixedwood	Coniferous	Herb	Wetland Treed	Broadleaf	Water	Wetland	Exposed Land	Total	User's Accuracy (%)	Commission Error (%)
PREDICTED	Mixedwood	0.336	0.020	0.013	0.020	0.007	0	0	0	0.397	84.75%	15.25%
	Coniferous	0.027	0.274	0.020	0	0	0	0	0	0.320	85.42%	14.58%
	Herb	0.014	0	0.077	0	0	0	0	0	0.090	84.62%	15.38%
	Wetland Treed	0.009	0	0	0.059	0	0	0.005	0	0.073	81.25%	18.75%
	Broadleaf	0.004	0	0	0	0.051	0	0	0	0.055	92.86%	7.14%
	Water	0	0	0	0	0	0.039	0	0	0.039	100.00%	0.00%
	Wetland	0	0	0	0.002	0	0	0.014	0	0.016	85.71%	14.29%
	Exposed Land	0	0	0.001	0	0	0	0	0.008	0.009	85.71%	14.29%
	Total	0.390	0.294	0.111	0.082	0.058	0.039	0.018	0.008	1		
	Producer's accuracy (%)	86.24%	93.13%	68.74%	72.50%	88.40%	100.00%	75.05%	100.00%	Overall accuracy		85.77%
	Omission error (%)	13.76%	6.87%	31.26%	27.50%	11.60%	0.00%	24.95%	0.00%	Margin of error ±		5.19%

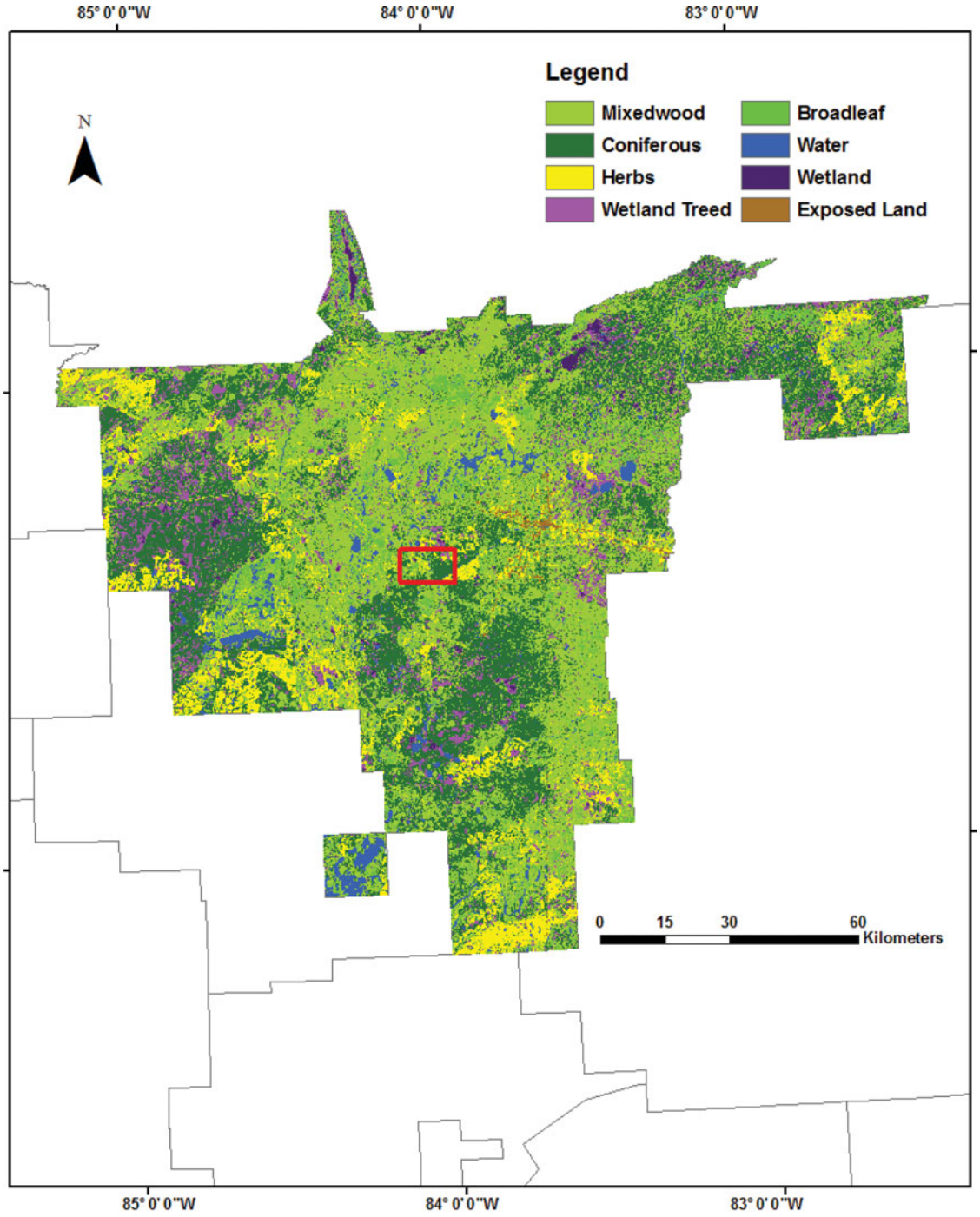

FIG. 4. Eight-class land cover classification in 2007 of the Hearst Forest study area in northern Ontario based on Landsat spectral data and time series disturbance metrics. Overall land cover classification accuracy was approximately 86% based on 174 reference sites. The small window outlined at the center of the map is the area shown in more detail in Figures 6, 7, and 8.

land cover change); of these, many of the land cover transitions were made to the herb land cover class from one of the forest classes. This occurred in each 5-year epoch. For example, of the 408 hectare mixedwood identified as having changed in the first epoch (in Table 8a), approximately 28.61% remained as mixedwood at the end of the epoch (despite having undergone a change in land cover class typically during the earlier part of the epoch). Another approximately 51.6% of this area, originally classified as mixedwood, changed to herb in the first epoch. Similarly, of the areas that began the first

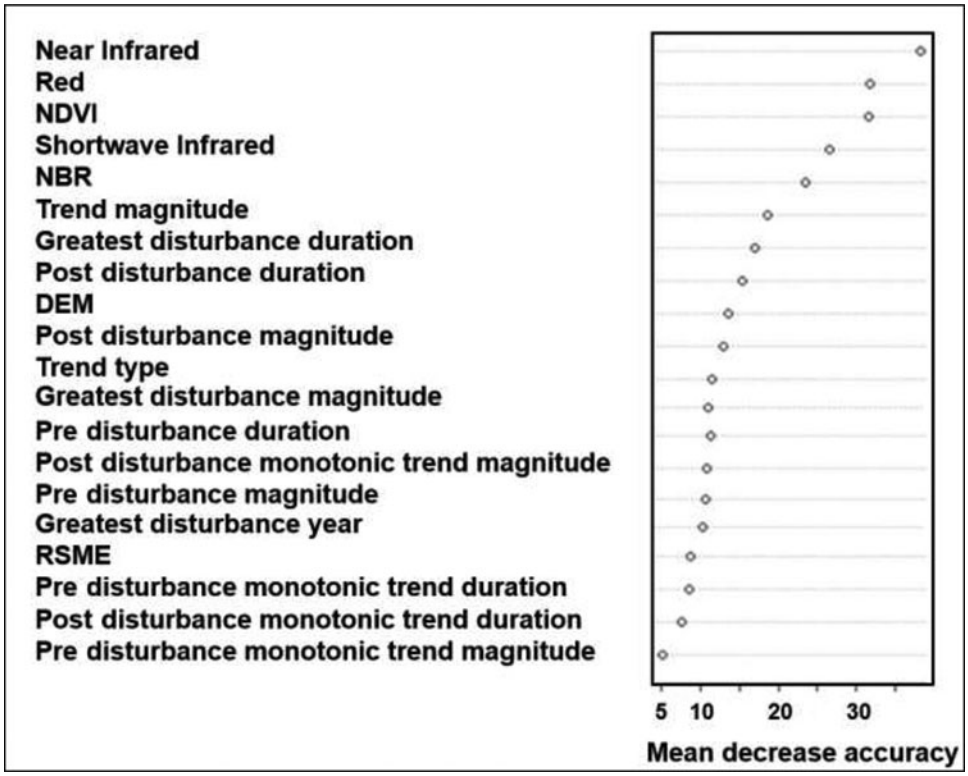

FIG. 5. Training data variable importance (VI) as estimated in the RF classifier; VI is the average of the squared classification error when the variable in the classification is replaced (permuted) with a random one and is an indication of the variables' contribution to the classification accuracy.

5-year epoch as conifer, and experienced a land cover transition during this epoch, approximately 23.9% returned to conifer by the end of the time epoch in 1995. In the same epoch, approximately 10.19% and 56.53% of these conifer land cover change pixels changed land cover to the mixedwood and herb classes, respectively. The exposed land cover pixels also show a reasonable land cover change trend over the first epoch; of the 25.8 hectare that began the first 5-year epoch classified as exposed

TABLE 6
Illogical class transitions used in the transition-rule filter. Acceptable class transition in the center year between the start and end year class is indicated with "√"; illogical transitions are indicated with "✗"

		Middle (second) year							
	Class	Mixedwood	Coniferous	Herb	Wetland Treed	Broadleaf	Water	Wetland	Exposed Land
Start (first) and end (third) year	Mixedwood	√	✗	√	✗	✗	✗	✗	✗
	Coniferous	✗	√	✗	✗	✗	✗	✗	✗
	Herb	√	✗	√	✗	✗	✗	✗	√
	Wetland Treed	✗	✗	✗	√	✗	✗	✗	✗
	Broadleaf	✗	✗	✗	✗	√	✗	✗	✗
	Water	✗	✗	√	✗	✗	√	√	√
	Wetland	✗	✗	√	✗	✗	√	√	√
	Exposed Land	✗	✗	√	✗	✗	√	√	√

TABLE 7

Error matrix of estimated area proportions for the transition-rule filtered land cover map for the reference year 2007. The classification for this map was performed using a combination of single date spectral variables and time series disturbance metrics (Table 1). Cell entries are expressed as the estimated proportion of area

		REFERENCE										
	Class name	Mixedwood	Coniferous	Herb	Wetland Treed	Broadleaf	Water	Wetland	Exposed Land	Total	User's Accuracy (%)	Commission Error (%)
PREDICTED	Mixedwood	0.343	0.013	0.013	0.020	0.007	0	0	0	0.397	86.44%	13.56%
	Coniferous	0.020	0.294	0.007	0	0	0	0	0	0.320	91.67%	8.33%
	Herb	0.014	0	0.077	0	0	0	0	0	0.090	84.62%	15.38%
	Wetland Treed	0.018	0	0	0.055	0	0	0	0	0.073	75.00%	25.00%
	Broadleaf	0.004	0	0	0	0.051	0	0	0	0.055	92.86%	7.14%
	Water	0	0	0	0	0	0.039	0	0	0.039	100.00%	0.00%
	Wetland	0	0	0	0.002	0	0	0.014	0	0.016	85.71%	14.29%
	Exposed Land	0	0	0.001	0	0	0	0	0.008	0.009	85.71%	14.29%
	Total	0.399	0.307	0.098	0.077	0.058	0.039	0.014	0.008	1		
	Producer's accuracy (%)	85.94%	95.62%	78.10%	70.87%	88.40%	100.00%	100.00%	100.00%	Overall accuracy		87.98%
	Omission error (%)	14.06%	4.38%	21.90%	29.13%	11.60%	0.00%	0.00%	0.00%	Margin of error ±		4.83%

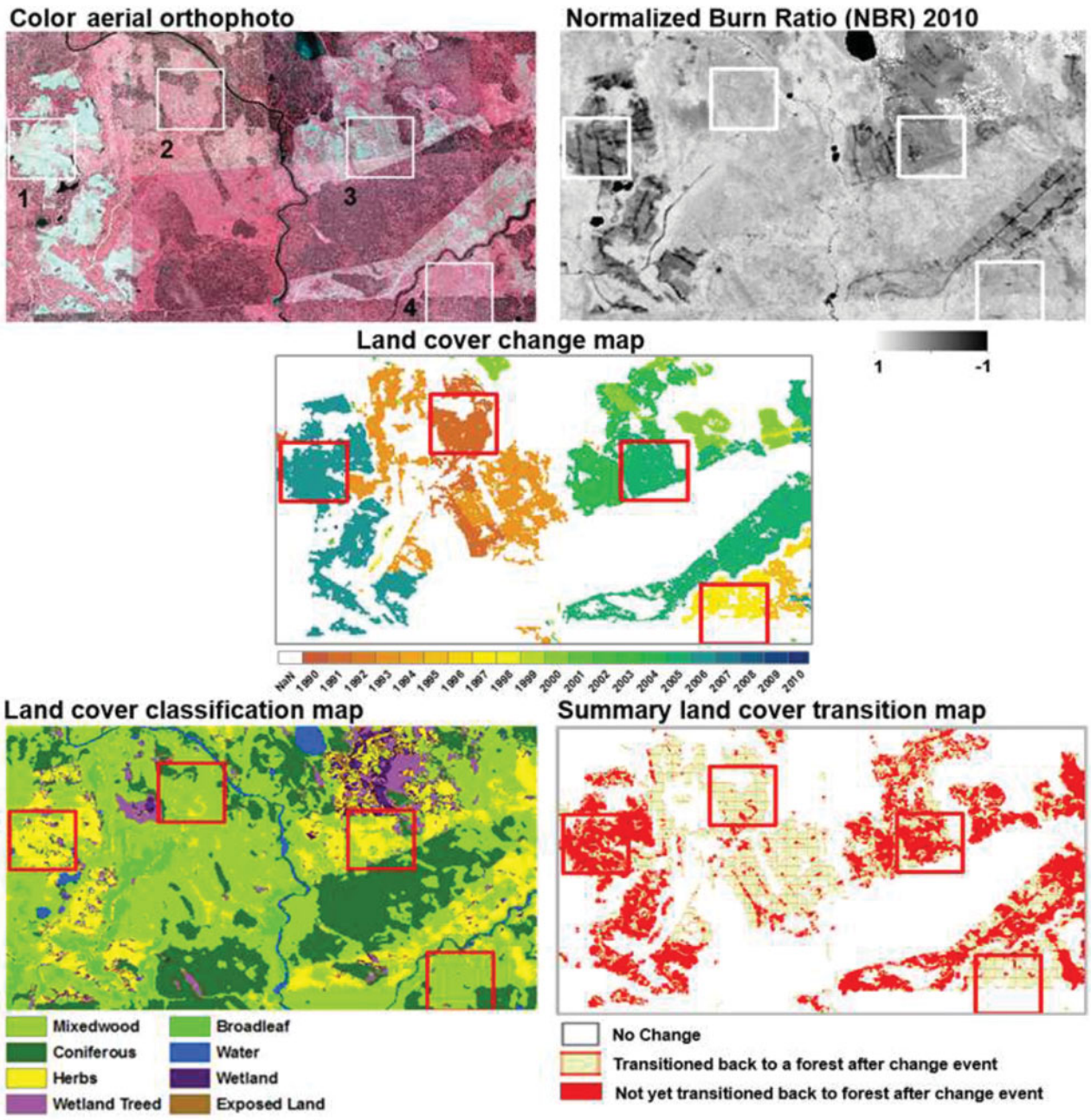

FIG. 6. A subarea of the Hearst Forest dataset showing exemplars of the various land cover transitions in the study area. Shown are the color-infrared aerial photography, normalized burn ratio (NBR), land cover changes over the 1990–2010 period, 8-class land cover classification for 2010, and a binary recovery no-recovery mask. Sites 2 and 4 were disturbed early in the time series 1991 and 1997, respectively; Sites 1 and 3 are more recent disturbances (2006 and 2005, respectively). Sites 2 and 3 are shown in greater detail in Figures 7 and 8, respectively.

land, approximately 34.23% experienced a land cover change (typically to the herb class) but remained or returned to the exposed land class by the end of the 5-year epoch. Approximately 16.2% and 35.99% of the exposed land pixels were classified as mixedwood and herb by the end of the first epoch.

There are clear patterns of change between mixedwood, coniferous, and herb land cover classes in each epoch and over the 20-year period. The transitions between these classes appear to represent land cover change and dynamics associated with harvesting activities (e.g., clearcutting conifer, to exposed,

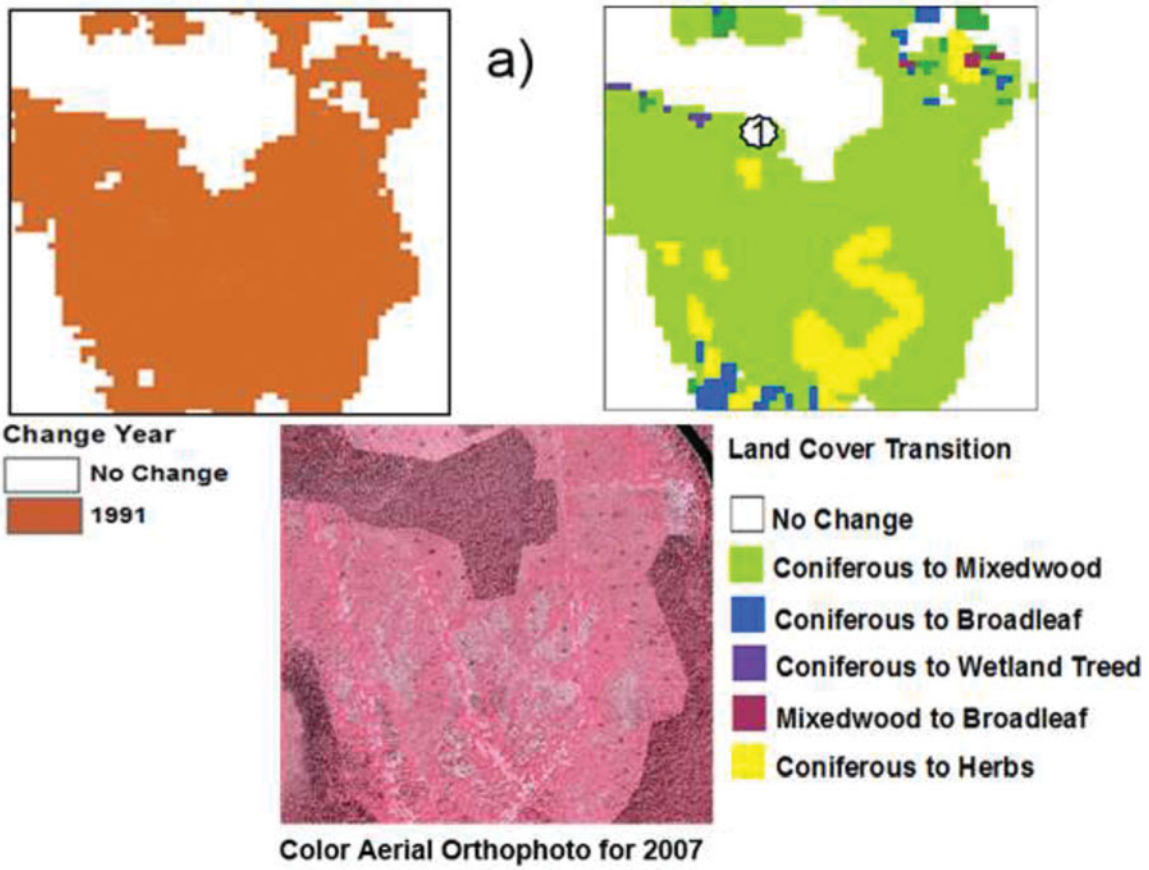

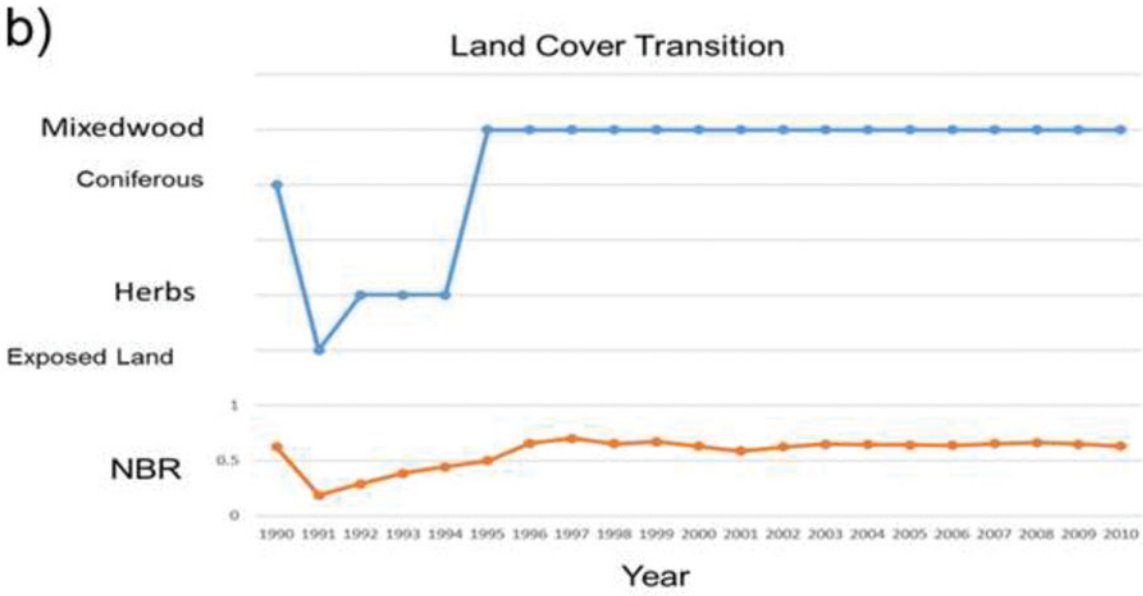

FIG. 7. Examples of land cover transitions in areas shown in Figure 6: (a) and (b) show Site 2, this site contains an area that was clearcut at the beginning of the available time series; at that time, the dominant land cover class was coniferous, and the majority of the area was converted to mixedwood at the end of the time period. The graph in 7(b) shows the land cover transitions for a pixel located near the edge of this cutover in Site 2 where the land cover has transitioned from coniferous to exposed land and then to herb and finally to mixedwood.

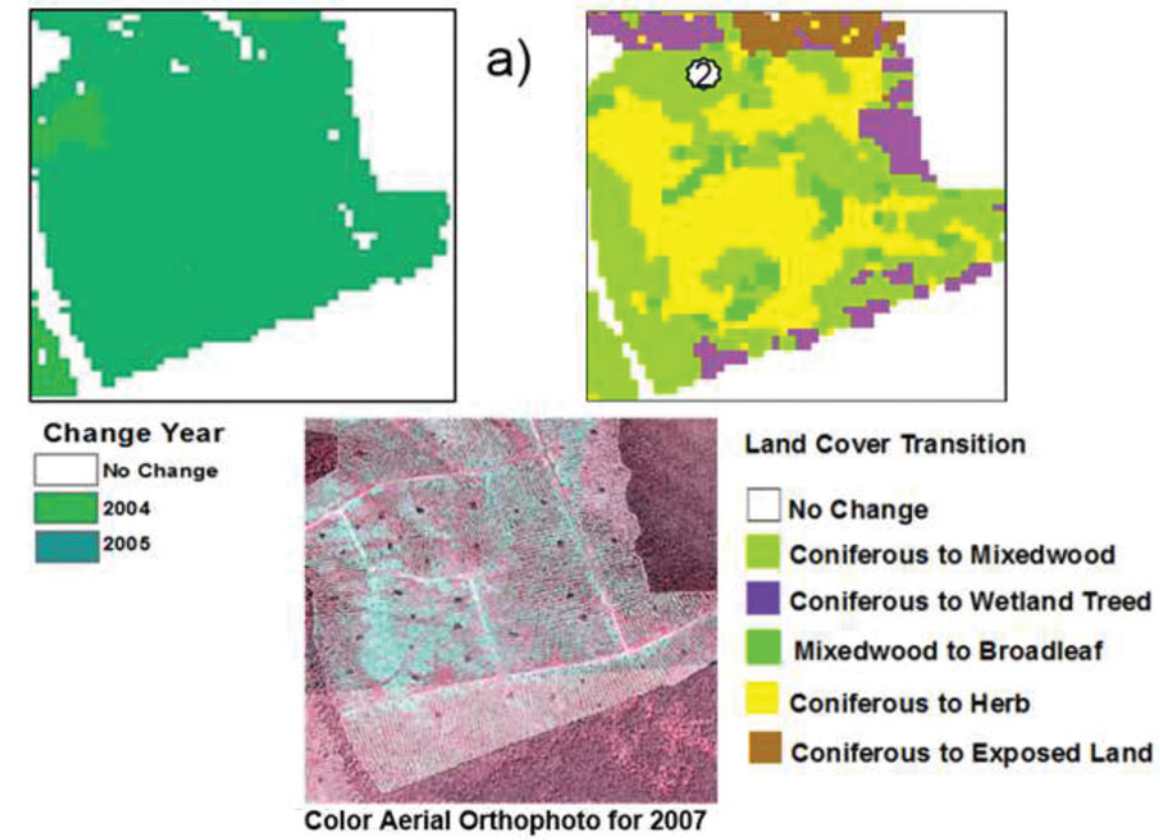

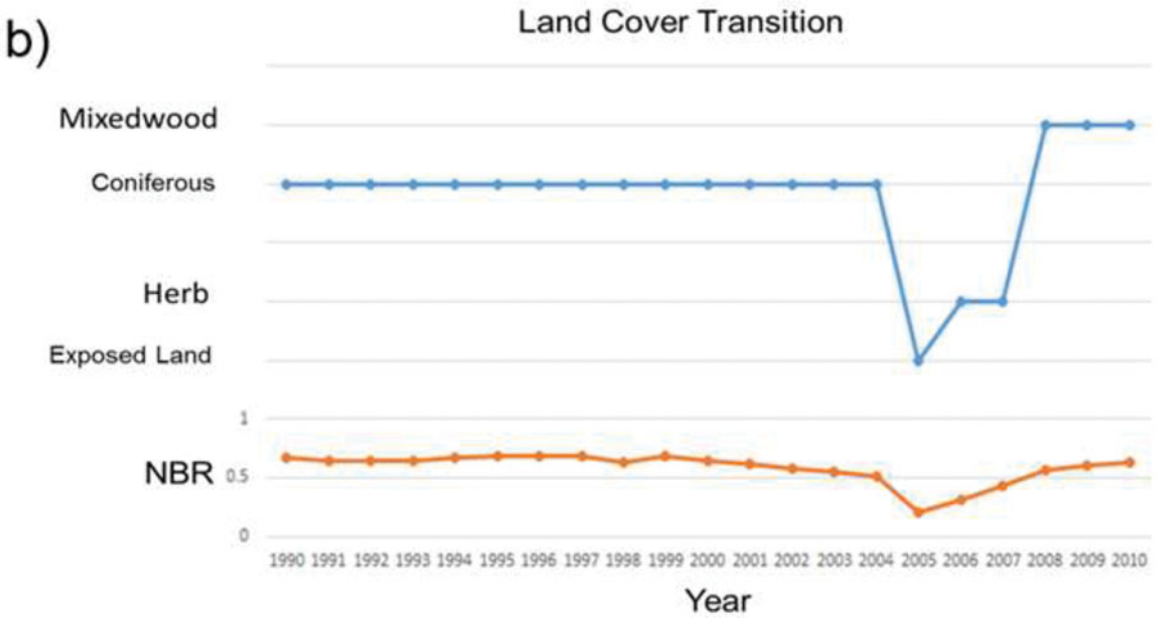

FIG. 8. Site 3 in Figure 6. Site 3 has experienced land cover change in 2004 and 2005, and many of these cutover pixels transitioned to different land cover classes by the end of the time series. The graph in 8(b) shows a pixel that began as conifer, transitioned to exposed land following harvesting, and subsequently transitioned from herb to mixedwood.

TABLE 8
Land cover class transitions (%) by 5-year epochs in the Hearst Forest

	Epoch 1 (1990–1995), Epoch 2 (1995–2000), Epoch 3 (2000–2005), Epoch 4 (2005–2010)						
	To						
From	Mixedwood	Coniferous	Herb	Wetland Treed	Broadleaf	Wetland	Exposed Land
Mixedwood							
Epoch 1	28.61	0.66	51.56	3.91	5.68	4.49	5.10
2	8.65	0.47	71.30	1.69	0.42	2.21	15.26
3	10.19	1.17	56.74	2.13	0.38	9.12	20.26
4	21.53	4.05	38.55	11.45	1.90	9.25	13.28
Coniferous							
Epoch 1	10.19	23.90	56.53	2.36	0.26	4.13	2.63
2	1.90	10.58	70.40	1.61	0.02	4.65	10.83
3	4.28	4.52	56.94	2.31	0.07	13.65	18.23
4	7.76	8.33	34.62	10.67	0.75	16.48	21.40
Herb							
Epoch 1	16.59	0.42	80.04	0.92	0.53	0.47	1.03
2	3.19	1.32	88.04	1.16	0.61	1.53	4.16
3	3.44	0.50	80.46	0.95	0.08	2.87	11.70
4	13.50	3.78	65.59	4.85	0.72	5.84	5.72
Wetland Treed							
Epoch 1	24.50	0.43	60.28	3.21	1.48	5.77	4.32
2	6.31	1.17	71.81	3.11	0.10	4.52	12.97
3	5.57	1.86	63.83	4.95	0.09	10.99	12.71
4	9.49	4.02	32.92	23.36	1.74	18.72	9.74
Broadleaf							
Epoch 1	28.16	0.17	49.55	0.73	6.16	5.94	9.29
2	5.33	0.18	73.62	0.24	3.46	2.39	14.77
3	7.52	0.26	51.47	1.38	32.54	1.89	4.92
4	10.62	6.06	56.31	3.44	4.67	6.08	12.81
Wetland							
Epoch 1	31.70	0.64	29.90	1.85	4.61	26.33	4.97
2	7.80	6.84	43.33	5.48	0.41	20.88	15.28
3	7.20	2.93	39.20	4.20	0.70	30.08	15.70
4	12.81	8.85	16.32	16.29	1.94	33.11	10.69
Exposed Land							
Epoch 1	16.20	0.27	35.99	1.09	3.21	9.01	34.23
2	2.21	1.38	19.75	0.71	3.59	1.12	71.24
3	2.20	0.37	29.45	0.89	0.21	2.13	64.76
4	6.88	1.12	46.89	4.57	0.87	4.31	35.36

to herb) and forest regeneration (e.g., herb to mixedwood). The annual land cover classification helps to confirm interpretations of the kind of land cover change occurring on an annual basis and over time for the entire study area. A compilation of the annual percentage of different land cover classes throughout the time series is contained in Figure 9. This classification method can be applied to other areas to produce spatially and temporally consistent information on annual land cover, providing sufficient archived Landsat data is available. The approach allows the use of spatially contiguous, cloud- and haze-free, spatially consistent, temporal series of Landsat data for large-area land cover mapping. The resulting information on land cover dynamics is important for the study of carbon modeling. Spatially explicit carbon modeling methods often require information on annual land cover and land cover changes, especially such that can be portrayed in a change matrix. The predisturbance land cover, the year of disturbance, and the postdisturbance land cover class information can be joined with data on carbon dynamics to esti-

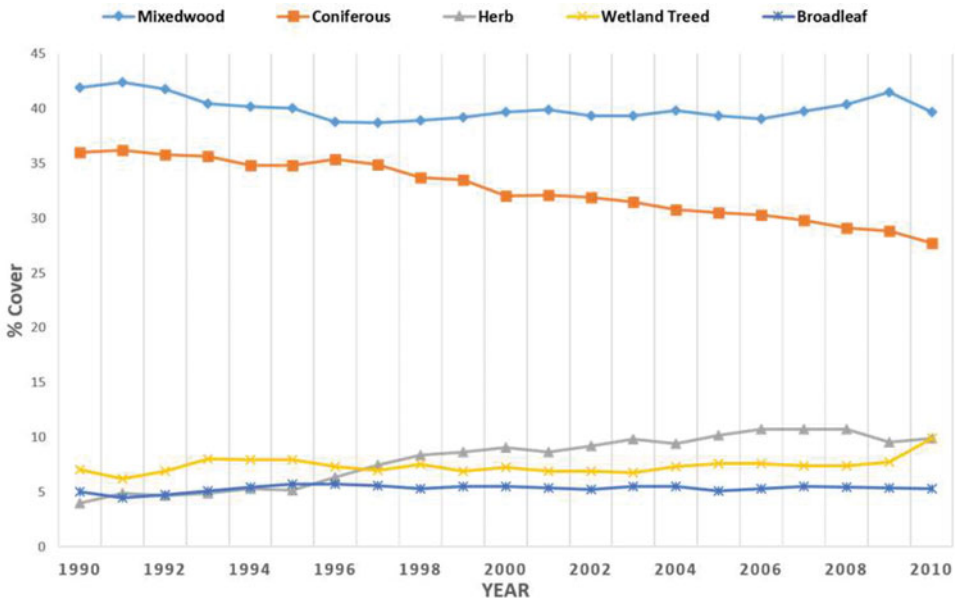

FIG. 9. Areal percentage of the 5 major land-cover classes mixedwood, coniferous, herb, wetland treed, and broadleaf for years 1990 to 2010.

mate carbon stocks, stock changes, and the associated emissions and removals over time. Future research is intended to implement land cover classification approaches using all available Landsat imagery to assess intra-annual phenological change and to test this approach for other regions with different environments. Further, knowing the variable yield of imagery that can be expected within a given year or growing season, opportunities such as those implemented by Senf et al. (2015), using multiscale applications, also merit additional investigation.

CONCLUSIONS

In this study, annual land cover maps were generated from a time series of Landsat image composites for the period 1990–2010 in the Hearst Forest in northern Ontario. Time series trajectory analysis identified areas that had changed land cover at least once during the 1990–2010 time period based on the greatest-change metric; such areas were then filtered for illogical transitions, examined for land cover change patterns, and interpreted in the context of known forest management practices and land cover transitions. Incorporation of change metrics derived from the time series into the land cover classification approach improved overall accuracy by 6.38% compared to single image-date results. Subsequent postclassification filtering of the time series of annual land cover classifications further improved overall accuracy by an additional 2.2%. The capacity to characterize land cover transitions through time is a unique contribution of this study. For example, mixedwood forest that experienced change early in the time series showed a typical vegetation transition pattern: mixedwood transitioned to exposed land following harvest, then transitioned to herb, and subsequently returned to mixedwood by the end of the time series. An area that was more recently disturbed changed from conifer to exposed land and then to herb. Such characterizations of land cover transitions rely on both the accurate detection of change events as well as the accurate classification of land cover. Future work will examine conversion of these transitions into inputs relevant for carbon budget modeling, such as predisturbance and postdisturbance land cover. These interpretations of land cover dynamics are also of general interest to monitoring, inventory, and reporting programs, as well as to characterizing postdisturbance recovery trajectories.

FUNDING

This research was supported by the Natural Science and Engineering Research Council of Canada and via the "Terrestrial Ecosystem Monitoring System project jointly funded by the Canadian Space Agency, Government Related Initiatives Program, and the Canadian Forest Service of Natural Resources Canada.

REFERENCES

Ahmed, O.S., Franklin, S.E., Wulder, M.A., and White, J.C. 2015. Characterizing stand-level forest canopy cover and height using Landsat time series, samples of airborne LiDAR, and the random forest algorithm. *ISPRS Journal of Photogrammetry and Remote Sensing*, Vol. 101, pp. 89–101. doi: http://dx.doi.org/10.1016/j.isprsjprs.2014.11.007.

Breiman, L. 2001. "Random forests." *Machine Learning*, Vol. 45; pp. 5–32.

Breiman, L., and Cutler, A. 2007. "Random forests—Classification description." *Random Forests*, accessed November 27, 2014, http://stat-www.berkeley.edu/users/breiman/RandomForests/cc_home.htm.

Card, D.H. 1982. "Using known map category marginal frequencies to improve estimates of thematic map accuracy." *Photogrammetric Engineering and Remote Sensing*, Vol. 49: pp. 431–439.

Cochran, W.G. 1977. *Sampling Techniques (3rd ed.)* New York, NY: John Wiley & Sons.

Czaplewski, R.L., and Patterson, P.L. 2003. "Classification accuracy for stratification with remotely sensed data." *Forest Science*, Vol. 49: pp. 402–408.

Dietterich, T.G. 2000. "An experimental comparison of three methods for constructing ensembles of decision trees: bagging, boosting, and randomization." *Machine Learning*, Vol. 40: pp. 139–157.

Genuer, R., Poggi, J.M., and Tuleau-Malot, C. 2010. "Variable selection using random forests." *Pattern Recognition Letters*, Vol. 31: pp. 2225–2236.

Goward, S.N., Masek, J.G., Cohen, W., Moisen, G., Collatz, G.J., Healey, S., et al., 2008. "Forest disturbance and North American carbon flux." *Eos*, Vol. 89: p. 11.

Hansen, M.C. and Loveland, T.R. 2012. "A review of large area monitoring of land cover change using Landsat data." *Remote Sensing of Environment*, Vol. 122: pp. 66–74.

Hearst Forest Management Inc. 2011. *Current Forest Condition*, accessed on April 20, 2014, http://www.hearstforest.com/english/current.html.

Hearst Forest Management Inc. 2007. *Forest Management Plan for the Hearst Forest*. Hearst, ON, Canada: Author.

Hermosilla, T., Wulder, M.A., White, J.C., Coops, N.C., and Hobart, G. 2015. "An integrated Landsat time series protocol for change detection and generation of annual gap-free surface reflectance composites." *Remote Sensing of Environment*, Vol. 158: pp. 220–234.

Huang, C., Goward, S.N., Masek, J.G., Thomas, N., Zhu, Z., and Vogelmann, J.E. 2010. "An automated approach for reconstructing recent forest disturbance history using dense Landsat time series stacks." *Remote Sensing of Environment*, Vol. 114: pp. 183–198.

Janssen, L.F., Jaarsma, J., and van der Linder, E. 1990. "Integrating topographic data with remote sensing for land-cover classification." *Photogrammetric Engineering & Remote Sensing*, Vol. 56: pp. 1503–1506.

Kangas, A. and Maltamo, M. (Eds.) 2006. "Managing forest ecosystems." In *Forest Inventory: Methodology and Applications.* Dordrecht, Netherlands: Springer.

Kennedy, R.E., Andréfouët, S., Cohen, W.B., Gómez, C., et al. 2014. "Bringing an ecological view of change to Landsat-based remote sensing." *Frontiers in Ecology and Environment*, Vol. 12: pp. 339–346. doi:10.1890/130066.

Kennedy, R.E., Cohen, W.B., and Schroeder, T.A. 2007. "Trajectory-based change detection for automated characterization of forest disturbance dynamics." *Remote Sensing of Environment*, Vol. 110: pp. 370–386.

Kennedy, R.E., Yang, Z., and Cohen, W.B. 2010. "Detecting trends in forest disturbance and recovery using yearly Landsat time series: 1. LandTrendr—Temporal segmentation algorithms." *Remote Sensing of Environment*, Vol. 114: pp. 2897–2910.

Lambin, E., et al. 2003. Dynamics of land use and land cover change in tropical regions. *Annual Review of Environment and Resources*, Vol. 28: pp. 205–241.

Liaw, A., and Wiener, M. 2002. "Classification and regression by random forest." *R News*, Vol. 2(No. 3): pp. 18–22.

Masek, J.G., Vermote, E.F., Saleous, N.E., Wolfe, R., Hall, F.G., Huemmrich, K.F., et al. 2006. "A Landsat surface reflectance dataset for North America, 1990–2000." *IEEE Geoscience and Remote Sensing Letters*, Vol. 3(No. 1): pp. 68–72.

Olofsson, P., Foody, G.M., Stehman, S.V., and Woodcock, C.E., 2013. "Making better use of accuracy data in land change studies: estimating accuracy and area and quantifying uncertainty using stratified estimation." *Remote Sensing of Environment*, Vol. 129: pp. 122–131.

Olofsson, P., Foody, G.M., Herold, M., Stehman, S.V., Woodcock, C.E., and Wulder, M.A. 2014. "Good practices for estimating area and assessing accuracy of land change." *Remote Sensing of Environment*, Vol. 148: pp. 42–57. doi: 10.1016/j.rse.2014.02.015.

Pflugmacher, D., Cohen, W.B., and Kennedy, R.E. 2012. "Using Landsat-derived disturbance history (1972–2010) to predict current forest structure." *Remote Sensing of Environment*, Vol. 122: pp. 146–165.

R Development Core Team. 2014. *R: A Language and Environment for Statistical Computing*. Vienna, Austria: Author. http://www.R-project.org/.

Roy, D., Wulder, M., Loveland, T., Woodcock, C., Allen, R., Anderson, M., et al. 2014. "Landsat-8: science and product vision for terrestrial global change research." *Remote Sensing of Environment*, Vol. 145: pp. 154–172.

Schmidt, G.L., Jenkerson, C.B., Masek, J., Vermote, E., and Gao, F. 2013. *Landsat Ecosystem Disturbance Adaptive Processing System (LEDAPS) Algorithm Description*. U.S. Geological Survey Open-File Report 2013–1057, accessed March 10, 2014, http://pubs.usgs.gov/of/2013/1057/.

Senf, C., Leitao, P.J., Pflugmacher, D., van der Linden, S., and Hostert, P. 2015. "Mapping land cover in complex Mediterranean landscapes using Landsat: Improved classification accuracies from integrating multi-seasonal and synthetic imagery." *Remote Sensing of Environment*, Vol. 156: pp. 527–536. doi:10.1016/j.rse.2014.10.018.

Sexton, J.O., Urban, L.D., Donohue, M.J., and Song, C. 2013. "Long-term land cover dynamics by multi-temporal classification across the Landsat-5 record." *Remote Sensing of Environment*, Vol. 128: pp. 246–258.

Turner, D.P., Guzy, M., Lefsky, M.A., Ritts, W.D., Van Tuyl, S., and Law, B.E. 2004. "Monitoring forest carbon sequestration with remote sensing and carbon cycle modeling." *Environmental Management*, Vol. 33(No. 4): pp. 457–466.

White, J.C., and Wulder, M.A. 2013. "The Landsat observation record of Canada: 1972–2012." *Canadian Journal of Remote Sensing*, Vol. 39: pp. 455–467.

White, J.C., Wulder, M.A., Hobart, G.W., Luther, J.E., Hermosilla, T., Griffiths, P., Coops, N.C., Hall, R.J., Hostert, P., Dyk, A., and Guindon, L. 2014. Pixel-based image compositing for large area dense time series applications and science. *Canadian Journal of Remote Sensing*, Vol. 40: pp. 192–212.

Woodcock, C.E., Allen, R., Anderson, M., Belward, A., Bindschadler, R., Cohen, W., Gao, F., Goward, S.N., Helder, D., Helmer, E., Nemani, R., Oreopoulos, L., Schott, J., Thenkabail, P.S., Vermote, E.F., Vogelmann, J., Wulder, M.A., and Wynne, R. 2008. "Free access to Landsat imagery." *Science*, Vol. 320(No. 5879): p. 1011.

Wulder, M.A., Kurz, W., and Gillis, M. 2004. "National level forest monitoring and modeling in Canada." *Progress in Planning*. Vol. 61: pp. 365–381.

Wulder, M.A., Franklin, S., White, J.C., Linke, J., and Magnussen, S. 2006. "An accuracy assessment framework for large-area land cover classification products derived from medium resolution

satellite data." *International Journal of Remote Sensing*, Vol. 27: pp. 663–683.

Wulder, M.A., and Franklin, S.E. 2007. *Understanding Forest Dynamics: Remote Sensing and GIS Approaches*. Boca Raton, FL: Taylor and Francis.

Wulder, M.A. White, J.C., Cranny, M., Hall, R.J., Luther, J.E., Beaudoin, A., Goodenough, D.G., Dechka, J.A. Monitoring Canada's forests. 2008. "Part 1: Completion of the EOSD Land Cover Project." *Canadian Journal of Remote Sensing*, Vol. 34: pp. 549–562.

Wulder, M.A., White, J.C., Magnussen, S., and McDonald, S. 2008. "Validation of a large area land cover product using purpose-acquired airborne video." *Remote Sensing of Environment*, Vol. 106: pp. 480–491.

Wulder, M.A., J.C. White, and N.C. Coops. 2011. "Fragmentation regimes of Canada's forests." *The Canadian Geographer*, Vol. 55(No. 3): pp. 288–300.

Wulder, M.A., Masek, J.G., Cohen, W.B., Loveland, T.R., and Woodcock, C.E. 2012. "Opening the archive: How free data has enabled the science and monitoring promise of Landsat." *Remote Sensing of Environment*, Vol. 122: pp. 2–10.

Yemshanov, D., McKenney, D.W., and Pedlar, J.H. 2011. "Mapping forest composition from the Canadian National Forest Inventory and land cover classification maps." *Environmental Monitoring and Assessment*, Vol. 184: pp. 4655–4669.

Zhu, Z., and Woodcock, C. E. 2012. "Object-based cloud and cloud shadow detection in Landsat imagery." *Remote Sensing of Environment*, Vol. 118: pp. 83–94. http://dx.doi.org/10.1016/j.rse.2011.10.028.

Zhu, Z., and Woodcock, C.E. 2014. "Continuous change detection and classification of land cover using all available Landsat data." *Remote Sensing of Environment*, Vol. 144(No. 3): pp. 152–171.